Optics Letters

Stable high-reflection Be/Mg multilayer mirrors for solar astronomy at 30.4 nm

Vladimir N. Polkovnikov,[1,*] Nikolai I. Chkhalo,[1] Roman S. Pleshkov,[1] Nikolai N. Salashchenko,[1] Franz Schäfers,[2] Mewael G. Sertsu,[2] Andrey Sokolov,[3] Mikhail V. Svechnikov,[1] and Sergei Yu. Zuev[1]

[1]Institute for Physics of Microstructures RAS, GSP-105, 603950 Nizhny Novgorod, Russia
[2]Department of Nanooptics and Technology, Helmholtz-Zentrum Berlin, Albert-Einstein-Straße 15, D-12489 Berlin, Germany
[3]Department Precision Gratings, Helmholtz-Zentrum Berlin, Albert-Einstein-Straße 15, D-12489 Berlin, Germany
*Corresponding author: polkovnikov@ipmras.ru

Received 29 October 2018; revised 29 November 2018; accepted 29 November 2018; posted 7 December 2018 (Doc. ID 349379); published 4 January 2019

The He-II ($\lambda = 30.4$ nm) emission line is one of the spectral channels chosen to study solar corona. This Letter reports on investigations of novel beryllium (Be)/magnesium multilayer coatings which, when incorporated beneath a protective bilayer of aluminium and Be, ensure particularly high-reflection coefficients of up to 56%, a spectral width of $\Delta\lambda = 1.6$ nm ($\lambda/\Delta\lambda \approx 20$), and high temporal stability.

https://doi.org/10.1364/OL.44.000263

The transition layer from the solar chromosphere to the corona is characterized by a sharp temperature increase (10^4 to 10^6 K). This transition layer is characterized by intense emissions of various ions whose excitation energies belong to this temperature range. The emissions are dominated by the lines of the He-II ions that are found in the lowest areas of the transition layer (a region with temperatures around 8×10^4 K).

Some of the most important problems in solar physics relate to the understanding of the mechanism for heating the solar corona and how the principal temperature gradient occurs in the transition layer. Thus, most orbital solar missions are foreseen on recording radiation from the He-II ion ($\lambda = 30.4$ nm). Such solar missions include, for example, SDO, STEREO, SOHO, and TESIS. It is also planned to make available 30.4 nm recording channels in future missions, such as those of the Solar Orbiter [1], ARKA [2], and KORTES [3] probes.

The optical bases of the telescopes in the observatories under consideration are normal-incidence multilayer mirrors (MLMs). Most often, a Mo/Si structure [4,5] is used for such MLMs. The peak reflectance of these MLMs with an Ir capping layer reaches $R \approx 26\%$ at $\lambda = 30.4$ nm, while the spectral width (FWHM) of the reflection peak is $\Delta\lambda = 2.2$ nm [5].

Such a large value of $\Delta\lambda$ leads to the issue that, along with the radiation of the target He-II ion, the detector also records signals from the spectral lines of the FeXV ($\lambda = 28.4$ nm) and FeXVI ($\lambda = 33.5$ nm) ions. FeXV and FeXVI ions are formed in the outer regions of the solar corona at temperatures of around 2.5×10^6 K and, therefore, represent processes occurring in that region, rather than in the transition layer.

Another significant disadvantage of Mo/Si MLMs is their high (up to 50%) second-order reflectivity that falls to the neighborhood of the 17 nm wavelength. This area of the solar spectrum is dominated by the emission line of the FeIX ($\lambda = 17.1$ nm) and FeX ($\lambda = 17.5$ nm) ions; radiation is formed at the boundary between the corona and the transition layer at temperatures of around 10^6 K.

Reference [6] reports on Al/Mo/B_4C MLMs. The peak reflectance of these MLMs at a wavelength of 30.4 nm was 42% with a FWHM comparable with Mo/Si ($\Delta\lambda > 3$ nm). The second reflection order of such mirrors exceeds 20%. There is also a long-term stability of the reflection characteristics of these MLMs. However, due to a large value of $\Delta\lambda$, this structure does not effectively suppress the emission of the FeXV and FeXVI ion lines.

Magnesium (Mg)-containing MLMs have been examined as alternative structures. Mg, the absorption edge of which is at $\lambda_L = 25$ nm, is one of the most transparent materials at wavelengths greater than 25 nm. Therefore, MLMs based on Mg can potentially combine both a high reflectivity and spectral selectivity. The problem of second-order reflection is also solved due to the fact that in the spectral range of $\lambda < 25$ nm Mg has high absorption, and Mg-containing MLMs have low reflectance.

Theoretically, SiC/Mg, B_4C/Mg, and Si/Mg MLMs have reflectivities ~60%. Such mirrors have been studied experimentally, e.g., in Refs. [4,7–9]. In each case, two points were evident. First, there were significant differences between the experimental data and the theoretical calculations. Secondly, the reflective characteristics exhibited poor temporal stability. In particular, as reported in Ref. [7], it was not even possible to determine the actual value of the reflectivity R immediately after the mirror deposition. At the time of measurement, the reflectance of the Si/Mg MLMs had decreased to $R = 5.6\%$ at $\lambda/\Delta\lambda = 22$ and, for B_4C/Mg, to $R = 0.2\%$

at $\lambda/\Delta\lambda = 16$. By contrast, SiC/Mg MLMs are more stable; with an initial reflectance $R = 42 - 44\%$ ($\lambda/\Delta\lambda \sim 20$), it only decreased to 30% over the five years of recording reported in Ref. [9].

The problem of the difference between theoretical predictions and experimental data is most frequently attributed to the effect of intermixing of materials at the interfaces. Barrier layers have been used successfully to counter such intermixing [4,10,11]. To date, the best combination of peak reflectivity and spectral bandwidth was provided by the four-component $Si/B_4C/Mg/Cr$ structure proposed in Ref. [4], and was studied further in Ref. [12]. According to Ref. [12], immediately after the deposition, this MLM had values of $R = 46\%$ and $\Delta\lambda = 1$ nm. However, due to oxidation, during the first year, the value of R fell to 30%. It then remained at this level over several years of successive monitoring.

Thus, the use of barrier layers only partially resolves the problems associated with degradation of the reflectance characteristics over time. In this case, the determining factor is the high chemical reactivity of Mg, particularly its susceptibility to oxidation.

In Refs. [9,13], the problem of the temporal stability of the reflective characteristics of Mg-containing MLMs is solved by the deposition of a capping layer that prevents the oxidation of structures. The authors investigated the coating of Al, Si, and SiC. The deposition of capping layers initially leads to a slight decrease in the reflection coefficient. Nevertheless, the reflectance of protected MLM after long storage is significantly higher than that of uncoated structure.

However, the problem of obtaining desired reflective characteristics, combining high reflection and spectral selectivity, makes us look for new solutions.

As an attempt to fully or partially solve the above-mentioned issues of MLMs for solar missions at the He-II emission lines, this Letter is devoted to studying the reflective properties of Be/Mg MLMs optimized for the wavelength of 30.4 nm. Special attention is paid to the temporal stability of the reflection characteristics.

Be-based mirrors have long attracted attention, primarily due to the theoretical possibility of providing a reflectivity above 70% near the absorption edge of this element ($\lambda = 11.1$ nm) [14–16]. As a result of the studies, a peak reflection coefficient was reached at this wavelength of 70.2% with a theoretical limit of 75.6%. The possibility of reaching 72% at a wavelength of 13.5 nm was demonstrated in Ref. [17] for Mo/Be/Si mirrors.

The prospects of using Be as the scattering material in the range $\lambda > 17$ nm were first stated in Ref. [18]. Figure 1 shows the spectral dependencies of the real (δ) and imaginary (β) additions to the index of refraction ($n = 1 - \delta + i \cdot \beta$) of the most frequently used scattering materials for Mg-containing mirrors, compared to Be [19].

From these dependencies, it follows that Be, with its absorption close to that of silicon, is superior in terms of optical contrast to Mg $\delta_{\text{scatter}} - \delta_{\text{spacer}}$. Although silicon carbide features better scattering ability, its absorption is significantly higher than that of Be. Thus, based on this brief analysis of optical properties, Be appears to be the most attractive scattering material for use in Mg-containing MLMs.

The reflectivity curves for the wavelength range of 15–35 nm are calculated for the simulated ideal periodic structures Mo/Si, $Al/Mo/B_4C$, Si/Mg, and SiC/Mg и Be/Mg (Fig. 2). The layer thicknesses are optimized for the maximum reflectance at 30.4 nm (first reflection order). The number of periods $N = 60$; the incidence is normal. In addition, the figure shows the emission line positions for some ions of the solar corona.

Mo/Si MLM have the smallest reflectance (about 20%) and the worst spectral selectivity ($\lambda/\Delta\lambda < 10$) at a wavelength of 30.4 nm. Better spectral selectivity is characteristic of the Si/Mg MLM (reflectivity at wavelengths of 28.4 and 33.5 nm are 1.3% and 0.5%, respectively). However, its peak reflection

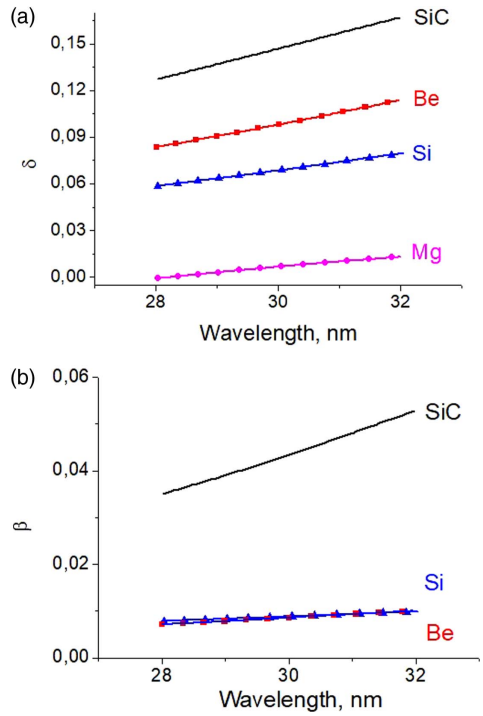

Fig. 1. Spectral dependencies of the index of refraction ($n = 1 - \delta + i \cdot \beta$) for (a) real and (b) imaginary additions.

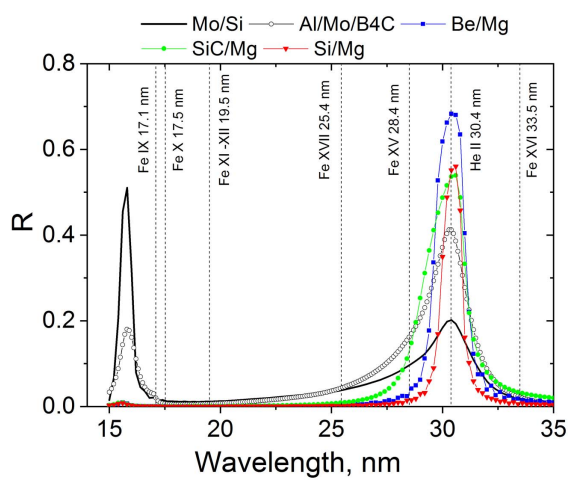

Fig. 2. Calculated spectral dependencies of the reflection coefficients of ideal Mo/Si, Al/Mo/B4C, Si/Mg, SiC/Mg, and Be/Mg MLMs optimized for maximum reflectance at $\lambda = 30.4$ nm. The period number is $N = 60$.

is considerably inferior to that of Be/Mg (56.8% versus 68.8%). The reflectances of the Be/Mg MLM at wavelengths of 28.4 and 33.5 nm are 2.3% and 1.6%, respectively, which are also acceptable for practical use.

Obviously, the second reflection order of Mg-free MLMs is high, while for Mg-containing MLMs the second reflection order does not exceed 1%. Thus, the use of Mg makes it possible not to take into account the lines of the corresponding ions and not to develop special absorption filters.

Be-containing MLMs were deposited in a specially certified laboratory, since Be is a highly toxic material. Be dust constitutes a threat to human health, and its effects have an accumulative nature. As far as deposited MLMs not producing small Be particles that can be breathed in, according to health and safety standards, the storage, research, and long-term operation of Be-containing MLMs are not harmful to human health, and these activities do not require special precautions [20].

Following the above theoretical analysis, MLMs were deposited onto super smooth (roughness RMS value of 0.1–0.2 nm) silicon substrates by means of magnetron sputtering. The sputtering was performed in an argon environment with 99.998% purity at a pressure of 0.1 Pa. The residual gas pressure did not exceed 10^{-4} Pa. The parameters of the structures (period, individual layer thickness, material density, and interlayer roughness) were determined by modeling to the measurements obtained at Philips X'Pert Pro diffractometer at a wavelength of $\lambda = 0.154$ nm. For fitting the reflectivity curves, IMD [21] software and an extended model were used [22].

Measurements in the vicinity of the 30.4 nm wavelength were performed both in the laboratory and at the BESSY-II synchrotron radiation center. A laboratory reflectometer with an LHT-30 grating spectrometer-monochromator (range: 25–200 nm, spectral resolution 0.1 nm) [23] and a gas discharge radiation source were used. Synchrotron measurements in the extreme ultraviolet range were performed at the Optics Beamline of BESSY-II with an 11-axis reflectometer [24]. The angular and spectral reflectivity dependencies for different MLMs were studied with fixed photon energy and with a fixed angle of the incident radiation.

Great attention was paid to issues of temporal stability of the reflective characteristics of the Be/Mg MLM. To assess this, between measurements some samples were stored in vacuum (pressure of the residual atmosphere about 100 Pa), while other samples were stored in room conditions.

Initially, two-component Be/Mg structures were studied. The parameters of the MLMs, obtained from reflectometry fits (thicknesses of individual layers and roughness), are $d_{\mathrm{Be}} = 6.51$ nm, $d_{\mathrm{Mg}} = 9.57$ nm, $\sigma(\text{Be-on-Mg}) = 0.35$ nm, and $\sigma(\text{Mg-on-Be}) = 0.85$ nm.

The reflectance of an as-deposited structure at a wavelength of 30.4 nm was 49% (angle of incidence of the radiation used was 5°). The significant difference between theoretically predicted and experimentally obtained reflection values may be explained by the presence of oxides in the structure. The temporal stability of the reflection characteristics of the $[\mathrm{Be/Mg}] \times 60/\mathrm{Be}_{6.5\,\mathrm{nm}}$ MLM is illustrated in Fig. 3, which shows the temporal dependence of the peak reflectance at a $\lambda = 30.4$ nm for two MLMs; one sample was stored at room conditions, and one was stored in vacuum.

As in the previously studied case of Mg-containing structures, a degradation of the reflectivity over time was observed.

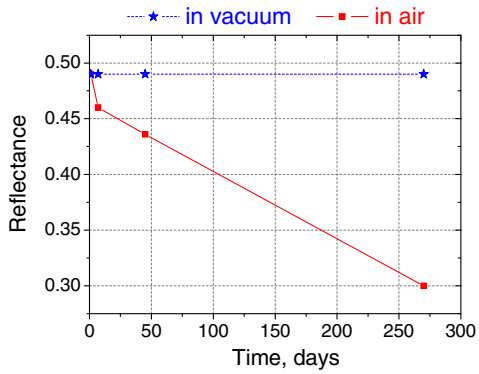

Fig. 3. Time dependence of uncoated $[\mathrm{Be/Mg}] \times 60/\mathrm{Be}$ 6.5 nm MLM reflectance at a wavelength of 30.4 nm for samples stored at room conditions (squares) and under vacuum (asterisks).

After nine months, it decreased from 49% to 30%. Based on the higher stability of the sample stored under vacuum, it can be concluded that the key factor resulting in degradation of the reflection coefficient is oxidation.

We studied several materials as the protective coatings. Initially, a top Be layer that was increased to 10 nm was tried. However, such a film did not perform the required protective functions: the reflectance of $[\mathrm{Be/Mg}] \times 60/\mathrm{Be}_{10\,\mathrm{nm}}$ MLM decreased by 2% during the month of observations.

In addition, the $MoSi_2$ film did not provide sufficient protection. Tests with films 3 and 5 nm thick were carried out. In the first case, the reflectivity loss over the month reached 4% while, in the second case, the loss was 1%. However, after nine months of observation, the loss exceeded 15% in both cases.

Following the idea proposed in Ref. [13], Al film was investigated as a protective layer. The best results showed a relatively thick (13 nm) Al film, deposited on the top Be layer of standard thickness (6.5 nm). If the top layer were Mg, the deposition of Al film on the top did not give the desired effect. Al and Mg do not form a sharp boundary, which can serve as a stop layer for atmospheric oxygen. Our research shows that the process of mixing Al and Mg at the border continues for a long time.

As shown in Ref. [18], due to the crystallization of Be and Al layers in Be/Al MLMs, it formed a rough (σ to 1.3 nm) but, in time, stable (the result of two-year observations of experimental samples) boundary. We believe that it turns out to be impervious to oxygen. However, in view of the possible diffusion of oxygen through gaps and interspaces in the crystallization of Be and Al layers, this statement needs additional research.

Studying the temporal stability of the reflection characteristics of $[\mathrm{Be/Mg}] \times 60/\mathrm{Be}_{6.5\,\mathrm{nm}}/\mathrm{Al}_{13\,\mathrm{nm}}$ MLMs revealed their stability (the difference did not exceed 0.005 and was comparable to the variation of the reflection coefficient across the sample surface) over nine months both for the sample stored under vacuum and for the one that remained in a normal atmosphere. Furthermore, this structure also had the highest reflectivity, $R = 56\%$, and a moderate passband, $\Delta\lambda = 1.6$ nm ($\lambda/\Delta\lambda \approx 20$).

Figure 4 shows the spectral dependency of the $[\mathrm{Be/Mg}] \times 60/\mathrm{Be/Al}$ MLM reflectance for both the sample stored in the atmosphere (symbols) and the sample kept under vacuum (solid line). The incidence angle of probing radiation was 2°. These curves were measured nine months after the MLM

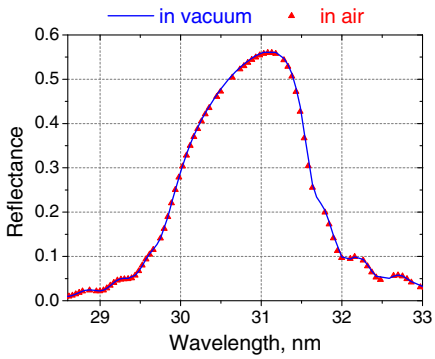

Fig. 4. Spectral dependency of [Be/Mg] × 60/Be 6.5 nm/Al 13 nm MLM reflectance for a sample stored in the atmosphere (symbols) and a corresponding sample kept under vacuum (solid line).

sputtering. Along with the FWHM value, it is important to note the measured reflectance at $\lambda = 28.4$ nm and $\lambda = 33.5$ nm was 1.2% and 2.3%, respectively.

Thus, the main result of our investigation is as follows. A new Be/Mg pair of materials has been proposed for use in the spectral region around 30 nm. The Be/Mg structure has a spectral reflection band of $\Delta\lambda = 1.6$ nm ($\lambda/\Delta\lambda \approx 20$), which is sufficient for suppressing nearby "satellite" lines. The use of a 13 nm thick Al film as a capping protective layer deposited on the top Be layer made it possible to obtain the particularly high-reflection coefficient of $R = 56\%$, while also stabilizing the structure. The observation of these mirrors for nine months did not reveal any degradation of their reflectivity. This indicates the great potential for the use of this pair of materials for future missions to study the sun. Despite the high reflective characteristics obtained and their temporal stability, in order to finally determine the prospects for using Be/Mg MLMs in space missions, we will continue observing samples stored in air and in vacuum for a few more years.

Funding. Russian Science Foundation (RSF) (16-42-01034, 17-12-01227); Deutsche Forschungsgemeinschaft (DFG) (SO 1497/1-1); Russian Foundation for Basic Research (RFBR) (16-07-00306, 17-02-00640, 17-52-150006, 18-02-00588, 18-32-00173).

Acknowledgment. We thank HZB for the allocation of synchrotron radiation beam time.

REFERENCES

1. D. Müller, R. G. Marsden, O. C. St. Cyr, and H. R. Gilbert, Sol. Phys. **285**, 25 (2013).
2. S. V. Kuzin, S. A. Bogachev, A. A. Pertsov, S. V. Shestov, A. A. Reva, and A. S. Ulyanov, Bull. Russ. Acad. Sci. **75**, 87 (2011).
3. S. V. Shestov, A. S. Ulyanov, E. A. Vishnyakov, A. A. Pertsov, and S. V. Kuzin, Proc. SPIE **9144**, 91443G (2014).
4. S. Yu. Zuev, S. V. Kuzin, V. N. Polkovnikov, and N. N. Salashchenko, Bull. Russ. Acad. Sci. **74**, 50 (2010).
5. A. J. Corso, P. Zuppella, P. Nicolosi, D. L. Windt, E. Gullikson, and M. G. Pelizzo, Opt. Express **19**, 13963 (2011).
6. E. Meltchakov, S. De Rossi, R. Mercier, F. Varniere, A. Jérome, F. Auchere, X. Zhang, M. Roulliay, and F. Delmotte, Proc. SPIE **8777**, 87771C (2013).
7. J. Zhu, S. Zhou, H. Li, Q. Huang, Z. Wang, K. Le Guen, M.-H. Hu, J.-M. André, and P. Jonnard, Appl. Opt. **49**, 3922 (2010).
8. P. Zuppella, A. J. Corso, P. Nicolosi, D. L. Windt, and M. G. Pelizzo, Proc. SPIE **8076**, 807608 (2011).
9. M. G. Pelizzo, A. J. Corso, P. Zuppella, P. Nicolosi, S. Fineschi, J. F. Seely, B. Kjornrattanawanich, and D. L. Windt, Opt. Eng. **51**, 023801 (2012).
10. H. Li, S. Zhou, Q. Huang, M. Tan, L. Jiang, J. Zhu, X. Wang, F. Wang, Z. Zhang, Z. Wang, and L. Chen, Proc. SPIE **7995**, 79951E (2011).
11. A. Aquila, F. Salmassi, Y. Liu, and E. M. Gullikson, Opt. Express **17**, 22102 (2009).
12. S. A. Bogachev, N. I. Chkhalo, S. V. Kuzin, D. E. Pariev, V. N. Polkovnikov, N. N. Salashchenko, S. V. Shestov, and S. Y. Zuev, Appl. Opt. **55**, 2126 (2016).
13. R. Soufli, M. Fernández-Perea, J. C. Robinson, S. L. Baker, J. Alameda, C. C. Walton, L. Rodríguez-De Marcos, J. A. Méndez, J. I. Larruquert, M. Vidal-Dasilva, and E. M. Gullikson, Proc. SPIE **8849**, 88490D (2013).
14. K. M. Skulina, C. S. Alford, R. M. Bionta, D. M. Makowiecki, E. M. Gullikson, R. Soufli, J. B. Kortright, and J. H. Underwood, Appl. Opt. **34**, 3727 (1995).
15. C. Montcalm, S. Bajt, P. B. Mirkarimi, E. A. Spiller, F. J. Weber, and J. A. Folta, Proc. SPIE **3331**, 42 (1999).
16. S. Bajt, J. Vac. Sci. Technol. A **18**, 557 (2000).
17. N. I. Chkhalo, S. A. Gusev, A. N. Nechay, D. E. Pariev, V. N. Polkovnikov, N. N. Salashchenko, F. Schäfers, M. G. Sertsu, A. Sokolov, M. V. Svechnikov, and D. A. Tatarsky, Opt. Lett. **42**, 5070 (2017).
18. N. I. Chkhalo, D. E. Pariev, V. N. Polkovnikov, N. N. Salashchenko, R. A. Shaposhnikov, I. L. Stroulea, M. V. Svechnikov, Y. A. Vainer, and S. Y. Zuev, Thin Solid Films **631**, 106 (2017).
19. B. L. Henke, E. M. Gullikson, and J. C. Davis, At. Data Nucl. Data Tables **54**, 181 (1993).
20. "ATSDR: Public Health Statement for Beryllium," https://www.atsdr.cdc.gov/PHS/PHS.asp?id=339&tid=33.
21. D. L. Windt, Comput. Phys. **12**, 360 (1998).
22. M. Svechnikov, D. Pariev, A. Nechay, N. Salashchenko, N. Chkhalo, Y. Vainer, and D. Gaman, J. Appl. Cryst. **50**, 1428 (2017).
23. S. S. Andreev, A. D. Akhsakhalyan, M. A. Bibishkin, N. I. Chkhalo, S. V. Gaponov, S. A. Gusev, E. B. Kluenkov, K. A. Prokhorov, N. N. Salashchenko, F. Schäfers, and S. Y. Zuev, Central Eur. J. Phys. **1**, 191 (2003).
24. F. Schäfers, H.-Ch. Mertins, A. Gaupp, W. Gudat, M. Mertin, I. Packe, F. Schmolla, S. DiFonzo, G. Soullie, W. Jark, R. P. Walker, X. Le Cann, R. Nyholm, and M. Eriksson, Appl. Opt. **38**, 4074 (1999).